Physica B 434 (2014) 145–148

Contents lists available at ScienceDirect

Physica B

journal homepage: www.elsevier.com/locate/physb

Instability of supersonic crack in graphene

Bin Zhang*, Gang Yang, Heming Xu

State Key Laboratory of Mechanics and Control of Mechanical Structures, and College of Aerospace Engineering, Nanjing University of Aeronautics and Astronautics, Nanjing 210016, China

ARTICLE INFO

Article history:
Received 24 September 2013
Received in revised form
31 October 2013
Accepted 13 November 2013
Available online 20 November 2013

Keywords:
Instability of crack
Graphene
Molecular dynamics simulations

ABSTRACT

The velocity and instability of crack motion in 2D hexagonal lattice of graphene under pure opening loads are investigated by atomistic molecular dynamics simulations. The brittle crack along zigzag direction in a strip can propagate supersonically at even 8.82 km/s under uniform normal loading of edge displacements. Crack moving straightly at low speeds produces atomically smooth edges, while kinking occur beyond a critical speed around 8.20 km/s equivalent to 65% of Rayleigh-wave speed in graphene, which validates previous theoretical predictions of rapid fracture instability in elastodynamics, and rough and irregular edges with oscillatory overhangs are formed subsequently.

1. Introduction

Dynamic fracture in brittle materials has been the object of much interest [1,2]. It is predicted in continuum mechanics that velocity of crack propagation under opening loads (mode-I) cannot exceed longitudinal wave speed. Moreover, materials are essentially discrete systems of atoms, and crack propagation speed depends upon the material microstructure [3]. Molecular dynamics (MD) simulations showed that a model-I crack could travel at super Rayleigh-wave speed V_r if locally stiffening hyperelasticity could occur at crack tip [1], in which a simple model of atomistic material is employed allowing systematic transition of interatomic potential from linear elastic to strongly nonlinear, and the straight crack starts to branch off at 0.73 V_r, comparable with the critical velocity of crack kinking obtained by Yoffe [4] using 2D linear elastic theory with no dissipation. The Yoffe instability is likewise reproduced theoretically [5]: cracks propagating along a straight line are unstable beyond a velocity of about 0.6 V_r, by modeling the elastic medium as a 2D triangular lattice of coupled springs. The interatomic potentials and lattice structures play essential roles in these models. Furthermore, cracks in brittle materials have terminal velocities far below theoretical predictions [6], and branching is a general phenomenon occurring in experimental work with either PMMA [6,7] or soda-lime glass [8], which has shown that a dynamic instability controls a crack's advance when its velocity exceeds a critical velocity of 0.36 V_r. With the existence of a critical point at which the velocity begins to oscillate, a new pattern is formed on the fracture surface [6]. A crack also changes locally its topology and sprouts small, microscopic side branches at the instability onset [9].

However, the above theoretical models are seldom examined in a 'real 2D material', such as graphene, an excellent candidate as a perfect hexagonal lattice [10,11]. Previous MD simulations [12] on graphite sheet (graphene) with inserted zigzag notch under constant applied strain show that crack propagates stably at an average speed of 6.2 km/s, ~50% of the calculated Rayleigh-wave speed (~12.4 km/s), but that retention of the cutoff function of early version potential makes the quantities of results questionable. Tearing suspended monolayer graphene membranes was ever explored by high-resolution transmission electron microscopy (HRTEM) [13]. Nevertheless, radiation damage by electron-beam energy and applied dose cannot be neglected for light element materials, such as carbon, due to the limitations of HRTEM [14]. It is still very difficult to measure experimentally the cracking speed of graphene under pure mechanical loading without electromechanical coupling effects, thus numeric or atomistic calculations would be the only access due to the microscopic size and rapid velocity of the moving crack-front.

So far, the speed and instability of crack growth in brittle graphene of hexagonal lattice are rarely considered in previous works regarding energy dissipation. Herein we conduct extensive MD simulations on dynamic rapid fracture of graphene under opening loads to address the aforementioned questions. The modified second-generation reactive empirical bond-order (REBO) potential [15] is used by shifting the cut-off distance and removing cut-off function to avoid unphysical dramatic increase in the interatomic force, while its nonlinearity remains. The evolution of atomically cleaving of graphene is then modeled without manually specified material constants.

* Corresponding author. Tel.: +86 13913811289; fax: +86 25 84891422.
E-mail addresses: beenchang@nuaa.edu.cn, been.chang@gmail.com (B. Zhang).

0921-4526/$ - see front matter © 2013 Elsevier B.V. All rights reserved.
http://dx.doi.org/10.1016/j.physb.2013.11.027

2. Simulation methodology

The well established REBO potential has been used elsewhere [16–18] to specifically describe the interatomic interaction of carbon atoms, by which the strong nonlinear of force-displacement relation under large deformation and the bond breaking or switching among multi-carbon atoms can be well represented. Two cutoff distances 1.7 Å and 2.0 Å are initially set for a smooth transition of cutoff function from 1.0 to 0.0 to bound the range of covalent interactions as the interatomic distance increases. However, such a cutoff function generates spurious bond forces near the cutoff distance, which will deduce unphysical results due to discontinuity in the second derivative of the cutoff function [19,20]. In this study, the cutoff function is taken to be 1.0 within a cutoff distance of 1.92 Å [21] and zero otherwise to avoid such artifact defects [18].

A strip model containing an initially straight crack is utilized [1]. The size of graphene slab is reasonably chosen in order to make all-atom simulations computationally efficient, shown in Fig. 1. Two rows of atoms are removed midway to generate seed cracks (notches) in our models, and the distance between two crack surfaces is big enough to avoid self sealing. More than 4000 carbon atoms in our slab model with its width $h=32.7$ Å and length $l=317.3$ Å are initially relaxed until the energy of the system is fully minimized at a specified temperature. As cracks along zigzag edges in graphene usually propagate self-similarly [18], we consider zigzag crack models only for study here. The original crack will advance under pure opening load of displacement Δh displaced away at strain rate $\dot{\varepsilon}=d(2\Delta h/h)/dt$. The thickness of graphene is assumed to be 3.34 Å under plane stress condition, hereafter, our results are normalized by 3.34 Å to make connection of a 2D sheet with 3D solid.

In addition, we implement the deformation-control method by applying uniform increment Δh of y-displacement (less than 0.16×10^{-2} Å per step) gradually to the top and bottom rigid edges while keeping x-displacement constrained in Fig. 1. At each applied load, the lattice structure is statically equilibrated to minimize the total energy by the BFGS geometry optimization algorithm [22], thereby configurations of local energy minima are obtained. The velocity-Verlet time stepping scheme is used with a time step 1 fs at predominantly 300 K coupled with a Berendsen thermostat. We note that MD simulations are often sensitive to the temperature control and the loading rate, thus our results mainly aim to provide a statistical qualitative understanding of the rapid fracture mechanism.

3. Results and discussion

In our numerical experiments of MD, initial cracks propagate instantly after threshold loading. As shown in Fig. 2, the crack grows with even edges at the beginning in a 'mirror' style, and accelerates rapidly. The position of crack tip is determined by finding the stable breakage of carbon bond ahead. The velocity $V=\Delta a/\Delta t$ at each crack length is measured over a possible small distance Δa (mostly one lattice spacing 2.46 Å for green lines and two for black lines in Fig. 2) at the crack tip within a time interval Δt. V increases sharply within a short crack distance once the crack is initiated, then reaches a position of dynamic equilibrium to fluctuate. This velocity fluctuation is due to topological defects formed randomly on the fresh edges accompanying with crack propagation, and also due to the discrete microstructure of graphene as the crack tip crosses one or more lattice spacing. As the crack is triggered after the breakage of carbon bond, the energy released from the potential energy stored around the tip is partly transformed into surface energy of creating new crack surfaces and partly dissipated into atomic motion, and then the energy flows in again under external work (mechanical energy density far ahead crack tip $\omega=0.5h\dot{\varepsilon}^2E/(1-\mu^2)$ in elastodynamics [23], where E is Young's modulus and μ is Poisson's ratio.). Meantime, the formation of topological defects induces lattice dispersion, which inevitably delays the crack growth.

The time scale associated with the atomic bond-breaking processes is smaller than that of the actual velocity fluctuation [7] that can be partly attenuated to a certain extent by averaging the velocity over a longer crack extension or time interval so as to emphasize the mean dynamics. Velocities illustrated by black curves in Fig. 2 are averaged over mostly two lattice spacing 4.92 Å, in which some noise fluctuations are swept off. The velocity fluctuates trivially with crack propagation, while the oscillations are amplified evidently at high strain rates ($\dot{\varepsilon}=4.898\times10^{-6}$ fs^{-1} to 1.959×10^{-5} fs^{-1}) leading to the increment of circumferential stress near vicinity of the crack tip, and instability appears, the crack tends to deviate from its straight path in Fig. 2(a)–(c). Once kinked, the crack edge becomes increasingly irregular, in a 'mist and hackle' style, and complicated with oscillatory overhangs, topological defects, and carbon chains bridging. The torn edges are similar to those in tapered nanoribbons of graphene [24].

Prior to evaluate the crack speed, we calculate the phase velocity of Rayleigh-wave V_r in graphene first. Assuming graphene is an isotropic elasticity, V_r can be approximated by $V_r\approx0.9194\ V_t$ for $\mu=0.25$ [25], where $V_t=(G/\rho)^{0.5}$ is the velocity of transverse wave, the density of graphene $\rho=2.30\times10^3$ kg/m^3. Recalling that $G=E/2(1+\mu)$, where $E=1.0$ TPa [26] and $\mu=0.165$ for graphene [27], we can estimate $V_r\approx12.56$ km/s for graphene, comparable with previous results [12].

The critical velocity of crack instability V_c is determined by averaging over possible small interval of crack increment before occurrences of kinking in Fig. 2(a)–(c). Therefore, $V_c\approx8.20$ km/s at $\dot{\varepsilon}=4.898\times10^{-6}$ fs^{-1}, 9.796×10^{-7} fs^{-1} and 1.959×10^{-5} fs^{-1},

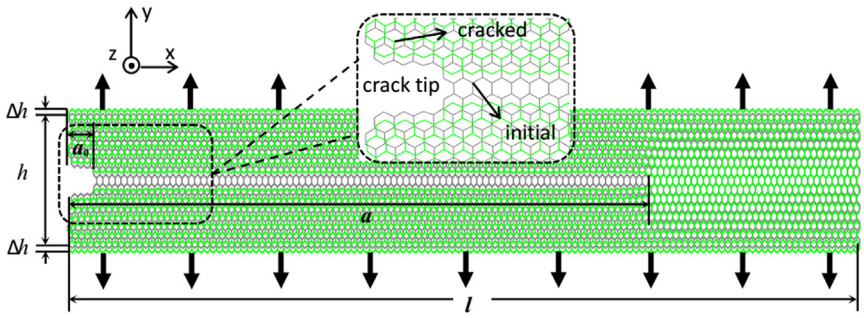

Fig. 1. The initial slab of graphene (grey lattice) overlapped with cracked strip (green) under uniform opening load of displacement (depicted by dark arrows on both top and bottom rigid sides that are constrained against displacement in x direction) Δh in y direction perpendicular to the crack line. The slab model occupies a width h and a length l with pre-inserted seed crack (snapshot) a_0 that extends to a along zigzag edges after loading. (For interpretation of the references to color in this figure legend, the reader is referred to the web version of this article.)

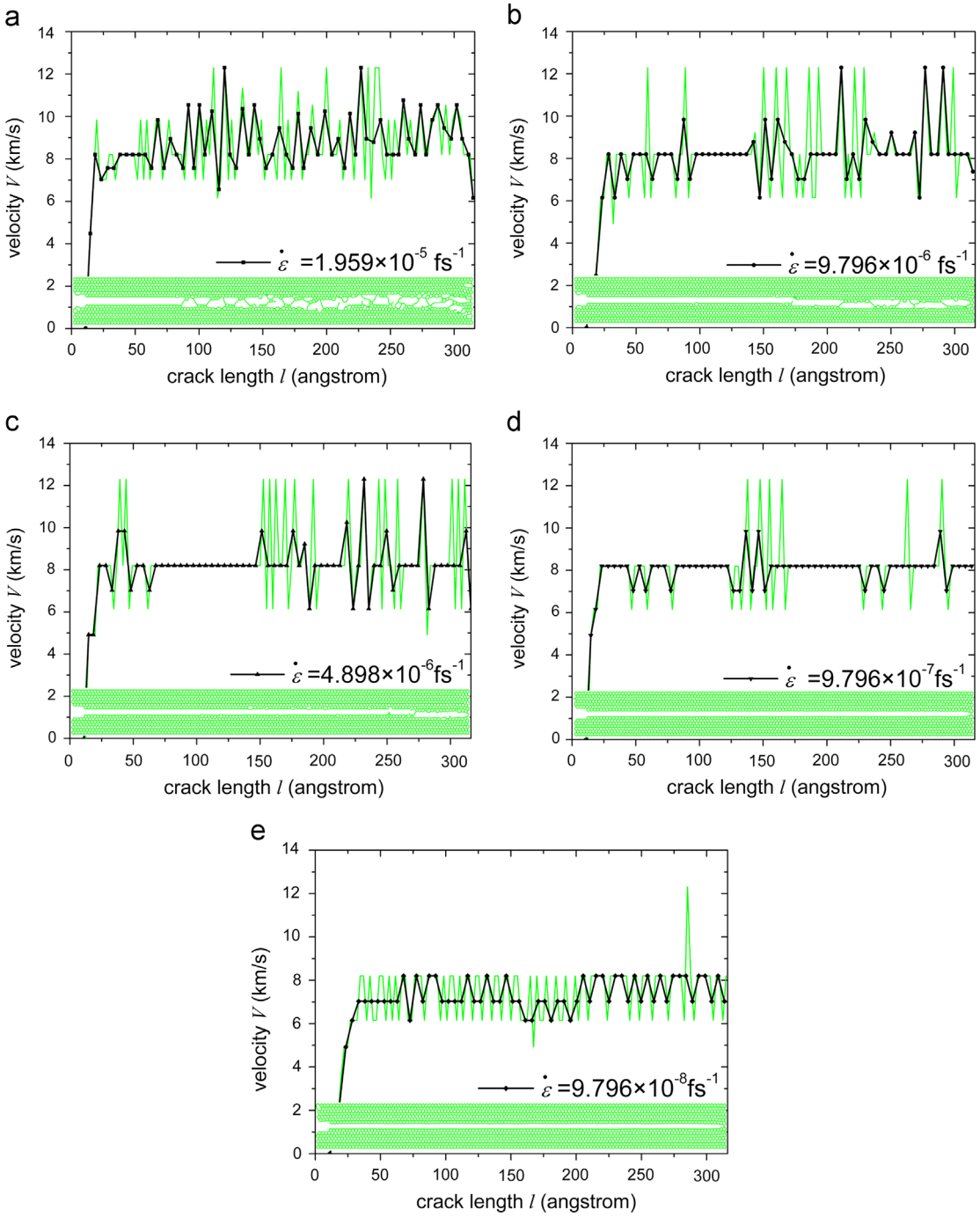

Fig. 2. Velocity and motion of crack in graphene. The velocity measurements are averaged over mostly two (black lines) or one lattice spacing 2.46 Å (green lines) within a time interval. Straight cracks start to kink beyond ~8.20 km/s, ~65% of the Rayleigh-wave speed (~12.56 km/s), which can be observed in the morphologies of fracture edges (green lattice snapshots at the bottom) in (a)–(c), while cracks undergo along straight lines enduringly without kinking at lower speeds in (d) and (e). (For interpretation of the references to color in this figure legend, the reader is referred to the web version of this article.)

respectively. As crack velocity should depend upon ω/γ in elastodynamic fracture [23,1], where $\gamma=1.041$ eV/Å [28] is facture surface energy of zigzag edge in graphene, we calculate ω_c/γ at critical strain ε_c that crack kinks, which yields $\omega_c/\gamma=0.132$, 0.121 and 0.127 TPaÅ^2/eV at $\varepsilon_c=9.1\%$, 8.6% and 8.9% respectively in Fig. 2(a)–(c). The uniformity of ω_c/γ indicates the consistency of above V_c that approaches 0.65 V_r (~12.56 km/s), coinciding with Yoffe's predictions of crack instability [4]. On the other hand, the crack tip energy release rate $0.5h\varepsilon_c^2\ E((1-(1-\mu^2)V_c^2\rho/E)/1-V_c^2\rho/E)$ [23] can be approached as 0.130, 0.119 and 0.125 TPaÅ with ε_c and V_c at the onset of instability, which is reasonably larger than the energy cost of breaking a graphene sheet, i.e. the surface energy $2\gamma=0.0997$ TPaÅ [28] (averaged over thickness 3.34 Å), providing that energy dissipation is considered. Furthermore, V_c is limited by V_r since the current nonlinear potential [15] allows strain softening at crack tips [2]. The crack kinking occurs earlier at higher strain rates, and vanishes at low rates, which can be noticed in the green lattice snapshots of crack motions in Fig. 2. The amplitude of velocity fluctuations narrows down with the mean velocity slowing down at low strain rates in Fig. 2(d) and (e), cracks propagate straightly and stably without branching, and the fracture edges are smoothly with 'mirror' character again.

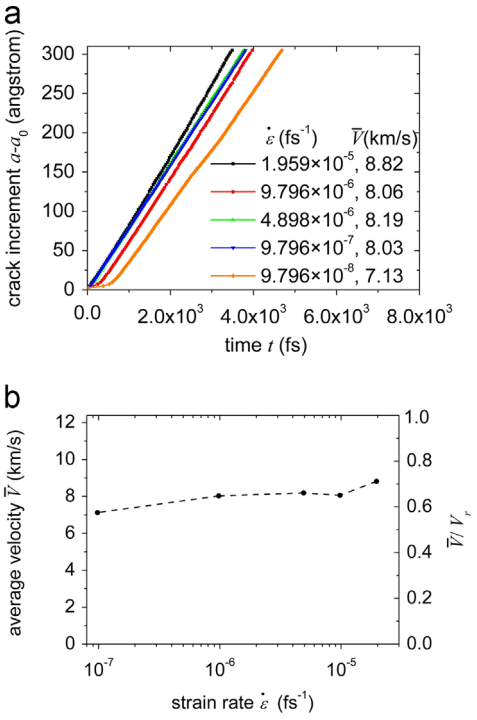

Fig. 3. The average velocity $\overline{V}$ (slope of $a-a_0 \sim t$ curve) over whole crack extension $l-a_0$. (a) Crack increment $a-a_0$ changes with propagating time t. (b) $\overline{V}$ on dependence of strain rate $\dot{\varepsilon}$. (For interpretation of the references to color in this figure legend, the reader is referred to the web version of this article.)

To eliminate the noise fluctuations of crack velocity, we average velocity over the whole length of crack extension. The average velocity $\overline{V}$ is measured by linearly fitting the $a-a_0 \sim t$ curves in Fig. 3(a), by which the slope $d(a-a_0)/dt$ is determined as $\overline{V}$ that falls in the range 7.13–8.82 km/s. $\overline{V}$ also increases with the strain rate of external displacement loading in Fig. 3(b). For the cases that crack kinks, the velocity $\overline{V} > 0.64\ V_r$, still consistent with Yoffe's instability and our previous predictions in Fig. 2(a)–(c).

The crack kinking occurs either downward or upward (not shown) in our simulations for the symmetry of both loading and geometry. Multiple branches are not observed in current models with zigzag cracks as that should be another aspect of crack instability under shearing [9,12,29]. Studies of fracture properties exhibited by graphene are in their infancy [30], and this intriguing research area would motivate further work.

4. Conclusions

We studied the crack velocity and instability in graphene strip under mode-I loads by faithful molecular dynamics calculations. The dynamic crack can move supersonically with a speed of even 8.82 km/s at high strain rate $1.959 \times 10^{-5}\ \mathrm{fs}^{-1}$ under boundary loading. Crack propagating straightly at low speeds leaves atomically flat edges along zigzag direction, while kinking and instability occur at speed exceeding ~8.20 km/s around 65% Rayleigh-wave speed ~12.56 km/s of graphene, and less smooth and irregularly rough edges are formed afterward. Our results lend further support for Yoffe's model of rapid crack instability in graphene.

Acknowledgments

This work was supported by NSFCs (11372131, 11232007 and 10602023), Aeronautical Science Foundation (2012ZF52074), 973 Program (2011CB707602), the Fundamental Research Funds for the Central Universities and the PAPD of China; Newton International Fellowship (NF080039) and Newton Alumni Follow-On of UK's Royal Society hosted by University of Glasgow and Newcastle University.

References

[1] M.J. Buehler, F.F. Abraham, H. Gao, Nature 426 (2003) 141.
[2] M.J. Buehler, H. Gao, Nature 439 (2006) 307.
[3] Y.J. Jia, W.P. Zhu, T. Li, B. Liu, J. Mech. Phys. Solids 60 (2012) 1447.
[4] E.H. Yoffe, Philos. Mag. 42 (1951) 739.
[5] M. Marder, X. Liu, Phys. Rev. Lett. 71 (1993) 2417.
[6] J. Fineberg, S.P. Gross, M. Marder, H.L. Swinney, Phys. Rev. Lett. 67 (1991) 457.
[7] J. Fineberg, S.P. Gross, M. Marder, H.L. Swinney, Phys. Rev. B: Condens. Matter 45 (1992) 5146.
[8] S.P. Gross, W.D. McCormick, M. Marder, H.L. Swinney, Phys. Rev. Lett. 71 (1993) 3162.
[9] E. Sharon, S.P. Gross, J. Fineberg, Phys. Rev. Lett. 74 (1995) 5096.
[10] K.S. Novoselov, A.K. Geim, S.V. Morozov, D. Jiang, Y. Zhang, S.V Dubonos, I.V. Grigorieva, A.A. Firsov, Science 306 (2004) 666.
[11] H. Zhao, N.R. Aluru, J. Appl. Phys. 108 (2010) 064321.
[12] A. Omeltchenko, J. Yu, R.K. Kalia, P. Vashishta, Phys. Rev. Lett. 78 (1997) 2148.
[13] K. Kim, V.I. Artyukhov, W. Regan, Y. Liu, M.F. Crommie, B.I. Yakobson, A. Zettl, Nano Lett. 12 (2012) 293.
[14] J.C. Meyer, F. Eder, S. Kurasch, V. Skakalova, J. Kotakoski, H.J. Park, S. Roth, A. Chuvilin, S. Eyhusen, G. Benner, A.V. Krasheninnikov, U. Kaiser, Phys. Rev. Lett. 108 (2012) 196102.
[15] D.W. Brenner, O.A. Shenderova, J.A. Harrison, S.J. Stuart, B. Ni, S.B. Sinnott, J. Phys. Condens. Matter 14 (2002) 783.
[16] B. Zhang., Physica B 418 (2013) 73–75.
[17] B. Zhang, Y. Liang, H. Sun, J. Phys. Condens. Matter 19 (2007) 346224.
[18] B. Zhang, L. Mei, H. Xiao, Appl. Phys. Lett. 101 (2012) 121915.
[19] O.A. Shenderova, D.W. Brenner, A. Omeltchenko, X. Su, L.H. Yang, Phys. Rev. B: Condens. Matter 61 (2000) 3877.
[20] T. Belytschko, S.P. Xiao, G.C. Schatz, R.S. Ruoff, Phys. Rev. B: Condens. Matter 65 (2002) 235430.
[21] R. Grantab, V.B. Shenoy, R.S. Ruoff, Science 330 (2010) 946.
[22] D.C. Liu, J. Nocedal, Math. Program. 45 (1989) 503.
[23] L.B. Freund, Dynamic Fracture Mechanics, second ed., Cambridge University Press, Cambridge, UK, 1998.
[24] D. Sen, KS Novoselov, PM Reis, MJ Buehler, Small 6 (10) (2010) 1108–1116.
[25] L. Rayleigh, Proc. London Math. Soc. 1 (1) (1885) 4–11.
[26] C. Lee, X. Wei, J.W. Kysar, J. Hone, Science 321 (2008) 385.
[27] O.L. Blakslee, D.G. Proctor, E.J. Seldin, G.B. Spence, T. Weng, J. Appl. Phys. 41 (1970) 3373.
[28] Q. Lu, R. Huang, Phys. Rev. B: Condens. Matter 81 (2010) 155410.
[29] A.L. Goff, P. Cobelli, G. Lagubeau, Phys. Rev. Lett. 110 (2013) 236101.
[30] I.A. Ovid'ko, Rev. Adv. Mater. Sci. 34 (2013) 1.